Proceedings Paper:
Afkhami, M, Hassanpour, A, Fairweather, M et al. (1 more author) (2013) Particle-Interaction Effects in Turbulent Channel Flow. In: Kraslawski, A, (ed.) Computer Aided Chemical Engineering. 23rd European Symposium on Computer Aided Process Engineering, 09-12 Jun 2013, Lappeenranta, Finland. Elsevier , 847 - 852. ISBN 978-0-444-63234-0

https://doi.org/10.1016/B978-0-444-63234-0.50142-1

Andrzej Kraslawski and Ilkka Turunen (Editors) Proceedings of the 23rd European Symposium on Computer Aided Process Engineering – ESCAPE 23 June 9-12, 2013, Lappeenranta, Finland,

Particle-Interaction Effects in Turbulent Channel Flow

M. Afkhami, A. Hassanpour, M. Fairweather, D.O. Njobuenwu

Institute of Particle Science and Engineering, School of Process, Environmental and Materials Engineering, University of Leeds, Leeds LS2 9JT, UK

Abstract

Large eddy simulation and a discrete element method are applied to study the flow, particle dispersion and agglomeration in a horizontal channel. The particle-particle interaction model is based on the Hertz-Mindlin approach with Johnson-Kendall-Roberts cohesion to allow the simulation of Van der Waals forces in a dry air flow. The influence of different particle surface energies on agglomeration, and the impact of fluid turbulence, are investigated. The agglomeration rate is found to be strongly influenced by the particle surface energy, with most of the particle-particle interactions taking place at locations close to the channel walls, aided by the higher concentration of particles in these regions.

Keywords: LES, DEM, particle, agglomeration, channel

1. Introduction

Understanding the fundamental aspects of turbulent fluid-particle flows is of relevance to processes employed in a wide range of applications, such as oil and gas flow assurance in pipes, powder dispersion in dry powder inhalers and particle re-suspension in nuclear waste ponds. Despite their importance, little is known about the influence of inter-particle collisions on the particle and fluid phase characteristics in the context of particle agglomeration, dispersion and deposition in such turbulent, bounded flows laden with large particle numbers. In this work, an advanced predictive technique for describing fluid motion, namely large eddy simulation (LES), is coupled with the discrete element method (DEM) to provide further understanding of such flows. A number of in-depth studies of pneumatic conveying through horizontal channels have been carried out in the past, such as those of Marchioli et al. (2008) as well as that of Lain and Sommerfeld (2012). The latter study, in particular, focuses on the effect of wall roughness on the particle concentration distribution across the channel and the velocity characteristics of both phases by accounting for full coupling between the phases. Pirker et al. (2010) also used a discrete element method coupled with fluid flow calculations and the Eulerian granular model to study horizontal conveying through a duct with a square cross-section. The emphasis in this work was related to the break-up of particle 'ropes' that consisted of very coarse particles (1 mm glass beads in this case) produced by a spiral inlet to the duct. However, the considered numerical approach did not give very good agreement with measurements regarding the particle mean velocity and volume fraction profiles along the duct. The present work is novel in linking the leading-edge predictive techniques of LES and DEM in predicting turbulent, particle-laden-channel flows. This coupled approach is capable of yielding fundamental insight into how particles interact in such flows, and how those interactions result in the formation of agglomerates which affect the dispersion and deposition of particles within the flow.

2. Numerical Simulations

The large eddy simulation employed a top-hat filter as this fits naturally into a finite-volume formulation. This decomposition is then applied to the Navier-Stokes equations for an incompressible Newtonian fluid with constant properties, bringing about terms which represent the effect of the sub-grid scale (SGS) motion on the resolved scale motions. The SGS stress model employed in this work was the dynamic model of Germano et al. (1996), and applied using the approximate localisation procedure of Piomelli and Liu (1995) in which the Smagorinsky model constant is dynamically computed based on the information provided by the resolved scales of motion. Computations were performed using the commercial CFD code ANSYS Fluent. The code implements an implicit finite-volume incompressible flow solver using a co-located variable storage arrangement. Because of this arrangement, a procedure similar to that outlined by Rhie and Chow (1983) is used to prevent checkerboarding of the pressure field. Time advancement is performed via an implicit method for all transport terms, and the overall procedure is second-order accurate in both space and time. Initially, an adaptive time-step was chosen, based on the estimation of a truncation error of 0.01 associated with the time integration scheme. If the truncation error was smaller than a specified tolerance, the size of the time- step was increased, and vice versa. This process continued until a constant time-step value was reached which was subsequently implemented as a fixed value. The code is parallel and uses the message passing interface HP MPI. Time-averaged flow field variables were computed from running averages during the computations. Further information on the mathematical model employed, and the numerical algorithm and its application, may be found in the ANSYS Fluent 13.0 theory guide.

An in-built Lagrangian approach was used to model particle motion from the instantaneous fluid velocity field in which the particles are tracked along their trajectories through the unsteady, non-uniform flow field. The particle-laden flow was assumed to be dilute (particle volume fraction ~ 10^{-5}), and the method incorporated full coupling between the phases, i.e. interactions between particles were considered, and the flow and particles were two-way coupled. Particle-wall collisions were assumed to be inelastic, with the coefficient of restitution set to 0.5. Particle-particle interactions were modelled using the discrete element method incorporating the contact model Herz-Mindlin with Johnson-Kendall-Roberts cohesion (Johnson et al., 1971) to allow the simulation of Van der Waals forces which influence the particle behaviour. The particle surface attractive force was altered by specifying the surface energy, with the amount of surface energy influencing the adhesion of the material. In this analysis, the aim was to minimize the number of degrees of freedom by keeping the simulation settings as simplified as possible; thus all particles were assumed to be rigid spheres with equal diameter and density, the effect of gravity was neglected, and particles much heavier than the fluid were assumed. Elghobashi and Truesdell (1993) have shown that the only significant forces in such systems are the Stokes drag and buoyancy forces, and that the Basset force can be neglected as it is an order of magnitude smaller. Buoyancy was also neglected in this work as the fluid was a gas. The shear induced Saffman lift force was taken into account as it considers non-trivial magnitudes in the viscous sub-layer.

3. Results and Discussion

The flow is described by a three-dimensional Cartesian co-ordinate system (x, y and z) representing the streamwise, spanwise and wall-normal directions, respectively. The boundary conditions for the momentum equations were set to no-slip at the channel

walls and the instantaneous flow field was considered to be periodic along the streamwise and spanwise directions, with a constant mass flux through the channel in the streamwise direction which was maintained by a dynamically adjusted pressure gradient used to drive the flow. The shear Reynolds number, $Re_\tau = hu\tau/v$, used in the simulations was 300, corresponding to a bulk Reynolds number of $Re_b \sim 8{,}400$. The rectangular channel considered was of dimensions $2h \times 2\pi h \times 4\pi h$, which in terms of wall units becomes $L_x^+ = 3547$, $L_y^+ = 1774$ and $L_z^+ = 563$. The length of the channel in the streamwise direction was sufficiently long to capture the streamwise-elongated, near-wall turbulent structures that exist in wall-bounded shear flows; such structures are usually shorter than ~ 1000 wall units. The non-uniform Cartesian grid used 1 million nodes (100×100×100). The initial particle positions were distributed randomly throughout the channel, corresponding to an initially uniform wall-normal particle number density profile. The initial particle velocity was set to 0 m s^{-1}, with the particles gradually coming in-line with local fluid velocities with time. Particles were assumed to interact with turbulent eddies over a certain period of time, that being the lesser of the eddy lifetime and the transition time. Particles that moved out of the rectangular channel in the streamwise and spanwise directions were re-introduced into the computational domain using periodic boundary conditions. The total number of particles considered in the computational domain was 20,000 in all cases. Particle and fluid densities were set to $\rho_p = 1000$ kg m^{-3} and $\rho_f = 1$ kg m^{-3}, respectively, with the kinematic viscosity set to $v = 15.7 \times 10^{-6}$ m^2 s^{-1}. The particle relaxation time is given by $\tau_p = \rho_p d_p^2/18\rho U$, and the non-dimensional particle response time is defined as the particle Stokes number, $St = \tau_p^+ = \tau_p/\tau_f$, where τ_f is a characteristic time scale of the flow (defined as $\tau_f = v/u_\tau^2$, where the shear velocity $u_\tau = 0.221$). Three particle surface energies were considered, with the corresponding particle relaxation times and Stokes number, and other relevant parameters, given in Table 1.

Surface Energy/J m^{-2}	d_p/μm	St (τ_p^+)	τ_p	τ_f
0.05, 0.5, 5.0	150	190	0.0612	0.000323

Table 1. Particle parameters used in the simulations.

The results generated by the LES for the fluid phase were verified using DNS predictions (Marchioli et al., 2008) for a shear Reynolds flow of $Re_\tau = 300$. Overall, the LES showed good agreement with the DNS, with the mean velocities and rms of fluctuating velocity components matching those of the DNS in both magnitude and position. The particle phase behaviour was also compared with one-way coupled DNS results, with the LPT incorporated in the commercial code giving results that were in reasonable agreement with those derived on the basis of the DNS.

Figure 1(a) shows results for the number of particle bonds in the channel with time. The results clearly illustrate a general increase in the number of bonds with time due to the effects of fluid turbulence on the particles; furthermore, the rate at which the particles form bonds increases with the particle surface energy, as would be anticipated. For the 0.05 J m^{-2} particles the rate of bond formation increases roughly linearly with time after an initial period. In the higher surface energy cases, however, the trend is highly exponential, indicating an ever increasing rate at which particle bonds form with time. Further scrutiny of the results, for all the particles, shows that agglomeration is first seen to occur at around t = 0.03 s; here the particles have increased their velocity to an extent where the fluid turbulence now causes particle-particle interactions. A linear increase in particle bond numbers then continues to about t = 0.1 s, after which an increasing

divergence is seen between the higher (5.0 and 0.5 J m^{-2}) and the lower (0.05 J m^{-2}) surface energy particles.

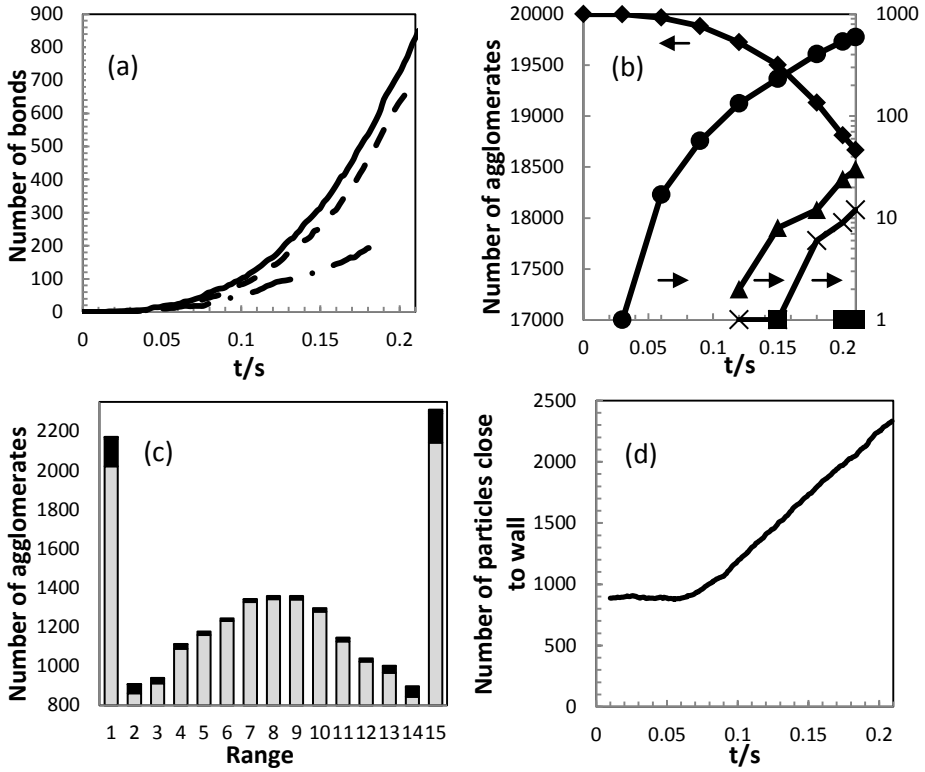

Figure 1. (a) Number of bonds between particles with time (—, ---, -·- surface energies of 0.05, 0.5 and 5.0 J m^{-2}, respectively); (b) number of particle agglomerates with time (♦, ●, ▲, ×, ■ single, double, triple, quadruple, quintuple agglomerates, respectively); (c) agglomerate distribution across the channel (□ single, ■ double-quintuple agglomerates, respectively); and (d) number of particles close to the wall with time (surface energy = 0.05 J m^{-2}).

This behaviour suggests that there is a phenomenon taking place within the channel that advantages the higher surface energy particles in the formation of agglomerates, other than the surface energy alone. This occurs as a result of regions of high particle concentration and low particle velocity near the channel walls; in such regions the number of bonds formed can be proportionally higher for particles of greater surface energy as the particle kinetic energy is sufficiently low to be ineffective in preventing particle separation after collision. Further analysis is required in order to establish a firmer relationship between particle surface energy and kinetic energy and their impact on the formation of successful Van der Waals bonds. The dispersing behaviour of the particles and the regions in which particle bonds are formed is, however, discussed further below. At the end of the simulation (t = 0.2s), and for the 0.05, 0.5 and 5.0 J m^{-2} surface energy particles, respectively, there are 195, 654 and 810 particle bonds in the flow. The greater surface energy of the 0.5 J m^{-2} particles compared to the 0.05 J m^{-2} particles, by one order of magnitude, therefore gives rise to more than three times the

number of bonds. However, a further increase of one order of magnitude in the surface energy to 5.0 J m^{-2} does not result in an equivalent increase in the number of bonds. This is indicative of the surface charge value nearing a threshold, hence, any further increase does not dramatically enhance particle agglomeration. From the above analysis, it is clear that the effects of fluid turbulence are dominant in creating particle-particle interactions, and that the particle surface energy is likewise a key factor in determining Van der Waals-induced particle agglomeration in the flow.

Figure 1(b) shows the time dependent number of particles within the agglomerates. In general, the number of single particles decreases gradually with time as the number of agglomerates increase with the simulation. For the single particles, there are initially 20,000, but this value begins to decrease at t = 0.03s and then follows a rapidly decreasing trend to 18,667 at t = 0.2s. The number of agglomerates of two particles is almost inversely proportional to the number of single particles, with these agglomerates forming first as t = 0.03s and increasing in number to a final value of 595 at t = 0.2s. The triple, quadruple and quintuple particle agglomerates first appear at t = 0.1, 0.12 and 0.15s, and increase to values of 30, 12 and 1 over the course of the simulation for the 5.0, 0.5 and 0.05 J m^{-2} surface energies, respectively. In this time frame, there are always far more double particles compared to triple and larger agglomerates, and this difference is seen to increase further with time. A much longer simulation time is also clearly required before significant numbers of triple and larger particle agglomerates can be formed. Based on these trends, however, it is clear that with time the number of agglomerates, and the size of the agglomerates, will continue to increase.

Figure 1(c) shows the relationship between the instantaneous position of the particles and agglomerates in the wall-normal direction for a particle surface energy of 0.5 J m^{-2}, and their number in this direction at a time t = 0.2s. Results are shown for 15 equally spaced regions across the channel, with particle statistics combined within each of the slabs of fluid considered. The location of each slab of fluid is represented by a column and plotted in relation to the channel walls, where columns 1 and 15 are the slabs adjacent to the bottom and top wall, respectively; these particular slabs have a width that stretches over 38 wall units representing the viscous sub layer ($y^+ < 5$) and the buffer layer ($5 < y^+ < 30$) within the near-wall region. The results show a general movement of particles and agglomerates (particle count) towards the walls, indicated by columns 1 and 15 which account for over $1/5^{th}$ of the total particle count. Closer examination of the results shows two opposing trends; a steady decrease in particle number from the centre of the channel (column 8) towards the walls up to and including slabs 2 and 14, followed by a dramatic increase in particle count at the walls. This likely indicates that particle numbers at the walls are directly related to the momentum of the particles prior to wall impact, such that higher velocity particles located in centre of the channel move towards the walls and rebound off them with a high velocity, then travelling back into the central region. In contrast, particles that drift towards the walls from regions of lower fluid velocity have less momentum and after impact with the wall become entrained in the near-wall region. Focusing on the agglomerates, the results clearly show an increase in their number towards the walls of the channel. At the channel centre, the fraction of the number of agglomerates to the total particle count is 0.012, although this value is seen to increase towards the walls, where for those slabs adjacent to the wall this value increases to 0.065 and 0.061. The number of agglomerates also increases uniformly towards the walls, in contrast to the total number count, bar in the final near-wall columns. Therefore, depending on the location of the agglomerates relative to the wall, two different conditions are responsible for their formation. Particle agglomeration near to the wall can therefore be attributed to a high

particle concentration, with the slabs closest to the wall showing the highest particle count and number of agglomerates. In the remaining regions, particle agglomeration is enhanced in high fluctuating fluid velocity fields which lead to a high number of particle-particle interactions. These velocity fluctuations are typically at a maximum 30 wall units away from the solid boundaries. This influence is indicated by the results for slabs 2 and 14, which contain the lowest particle count and yet the highest agglomerate number (bar those regions closest to the walls).

Lastly, Figure 1(d) shows the time evolution of the number of particles close to the wall. The results clearly show that from t = 0.06s particles accumulate at the wall at an approximately linear rate. From earlier work, it is known that for turbulent channel flows particle positions close to a wall correlate with instantaneous regions of low velocity along the streamwise direction, avoiding regions of high velocity, with the former defined as areas of lower-than-mean streamwise velocity (Pan and Banerjee, 1996). The behaviour demonstrated in Figure 1(d) is consistent with the findings reported in Marchioli et al. (2008) for flow in a channel, where turbophoresis causes the accumulation of particles in near-wall regions, which in the present flow clearly also enhances the rate of particle agglomeration in such regions.

4. Conclusions

The effect of surface energy and fluid turbulence on particle agglomeration has been studied in a channel flow. It has been found that the turbulent structure of the flow dominates the motion of the particles creating particle-particle interactions. A positive relationship between particle surface energy and agglomeration was also observed. The process of particle agglomeration was seen to be enhanced in two separate regions within the channel; in the near-wall region due to the high particle concentration driven by turbophoresis, and in the high turbulence regions close to the walls caused by the shearing effect of the flow at the no-slip boundaries.

References

M.F. Cargnelutti, L.M Portela, 2008, Statistics of Particle Dispersion in Direct Numerical Simulations of Wall-Bounded Turbulence, Int. J. Multiph. Flow, 34, 879-893.

M. Germano, U. Piomelli, P. Moin, W.H. Cabot, 1996, Dynamic Subgrid-Scale Eddy Viscosity Model, In Summer Workshop, Center for Turbulence Research, Stanford, CA, 1996.

K.L. Johnson, K. Kendall, A.D. Roberts, 1971, Surface Energy and the Contact of Elastic Solids, Proc. R. Soc. A, 324, 301-313.

S. Laín, M. Sommerfeld, 2012, Numerical Calculation of Pneumatic Conveying in Horizontal Channels and Pipes, Int. J. Multiph. Flow, 39, 105-120.

C. Marchioli, A. Soldati, J.G.M. Kuerten, B. Arcen, A.Tanière, G. Goldensoph, K.D.Squires, S. Elghobashi, G.C. Truesdell, 1993, On the Two-Way Interaction Between Homogeneous Turbulence and Dispersed Solid Particles, I: Turbulence Modification, Phys. Fluids A, 5, 1790-1801.

Y. Pan, S. Banerjee, 1996, Numerical Simulation of Particle Interactions with Wall Turbulence, Phys. Fluids, 8, 2733-2755.

U. Piomelli, J. Liu, 1995, Large Eddy Simulation of Rotating Channel Flows Using a Localized Dynamic Model, Phys. Fluids, 7, 839-848.

S. Pirker, D. Kahrimanovic, C. Kloss, B. Popoff, M. Braun, 2010, Simulating Coarse Particle Conveying by a Set of Eulerian, Lagrangian and Hybrid Particle Models. Powder Technol., 209, 203-213.

C.M. Rhie, W.L Chow, 1983, Numerical Study of the Turbulence Flow Past an Airfoil with Trailing Edge Separation, AIAA J., 21, 525-532.